Fermilab-Conf-08-209-APC   June 2008

ENERGY DEPOSITED IN THE HIGH LUMINOSITY INNER TRIPLETS OF THE LHC BY COLLISION DEBRIS[†]

E.Wildner, CERN, Geneva, Switzerland, F. Broggi, INFN, Sez. Milano – LASA, Segrate, Italy,
F.Cerutti, A. Ferrari, C. Hoa, J.-P. Koutchouk, CERN, Geneva, Switzerland,
N.V. Mokhov*, FNAL, Batavia, IL 60510, U.S.A.

Abstract

The 14 TeV center of mass proton-proton collisions in the LHC produce not only debris interesting for physics but also showers of particles ending up in the accelerator equipment, in particular in the superconducting magnet coils. Evaluations of this contribution to the heat, that has to be transported by the cryogenic system, have been made to guarantee that the energy deposition in the superconducting magnets does not exceed limits for magnet quenching and the capacity of the cryogenic system. The models of the LHC base-line are detailed and include description of, for energy deposition, essential elements like beam-pipes and corrector magnets. The evaluations made using the Monte-Carlo code FLUKA are compared to previous studies using MARS. For the consolidation of the calculations, a dedicated comparative study of these two codes was performed for a reduced setup.

ENERGY DEPOSITED IN THE HIGH LUMINOSITY INNER TRIPLETS OF THE LHC BY COLLISION DEBRIS

E.Wildner, CERN, Geneva, Switzerland, F. Broggi, INFN, Sez. Milano – LASA, Segrate, Italy,
F.Cerutti, A. Ferrari, C. Hoa, J.-P. Koutchouk, CERN, Geneva, Switzerland,
N.V. Mokhov, FNAL, Batavia, Illinois,U.S.A.

Abstract

The 14 TeV center of mass proton-proton collisions in the LHC produce not only debris interesting for physics but also showers of particles ending up in the accelerator equipment, in particular in the superconducting magnet coils. Evaluations of this contribution to the heat, that has to be transported by the cryogenic system, have been made to guarantee that the energy deposition in the superconducting magnets does not exceed limits for magnet quenching and the capacity of the cryogenic system. The models of the LHC base-line are detailed and include description of, for energy deposition, essential elements like beam-pipes and corrector magnets. The evaluations made using the Monte-Carlo code FLUKA are compared to previous studies using MARS. For the consolidation of the calculations, a dedicated comparative study of these two codes was performed for a reduced setup.

FLUKA-MARS COMPARISON

In order to compare energy deposition results with FLUKA 2006.3 [1,2] and MARS 15 [3], the configuration of the simulation models have to be exactly the same so the different results may only come from the physics of the codes [4].

Simplified IR5 model

The simplified geometry, representing the main features of the inner triplet quadrupole and IR5 layout, has cylindrical symmetry. It includes the copper collimator 'Target Absorber Secondaries (TAS)', the first quadrupole magnet Q1 and the stainless steel beam pipe in the magnet (Figure 1). The energy deposition in the superconducting cable is highest in the inner cable; it is close to the beam pipe. Both codes use the event generator DPMJET III [5] for simulating the proton-proton collisions.

Energy Deposition Results

- Normalization Factor

Both codes give the energy deposition in GeV/primary, in our case per proton-proton collision. The following formula (1) gives the transformation to power deposition, as a function of the luminosity L and the reaction cross section A (including inelastic scattering and single diffraction events):

$$Power = Energy*10^{9}*1.602*10^{-19}*L*A*10^{-24} \quad (1)$$

where Power is in W, Energy in GeV/collision, L in collisions·cm^{-2}s^{-1} and A in barn.

Equation (1), considering the upgrade LHC luminosity, L=10^{35}cm^{-2}s^{-1} , and assuming A= 80 mbarn, becomes:

$$Power[W] = 1.28*Energy[GeV/collision] \quad (2)$$

$$Power\ density[mW/cm^{3}] = 1280*Energy[GeV/cm^{3}/collision] \quad (3)$$
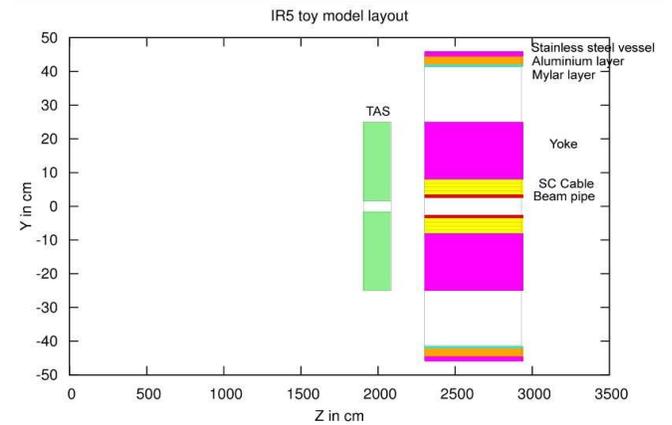

Figure 1: Layout for the comparison.

- Total heat loads

Table 1 presents the results of the total heat loads in the different components of the insertion region. The agreement between the two independent codes FLUKA and MARS is quite good, i.e., within less than 5% for most elements. In the most interesting region, the SC coil, the agreement is remarkable (within 1%). The yoke region shows a discrepancy of 23%, which can be attributed to differences in composition of the yoke material used in the models.

Table 1: Comparison of total heat loads (W),
upgrade luminosity L=10^{35}cm^{-2}s^{-1}

IR Elements	FLUKA	MARS
TAS	1853.7	1827.3
Beam pipe	89.1	97.9
Q1 cable	158.0	159.1
Q1 yoke	96.3	78.5
Aluminium layer	2.3	2.4
Insulation	19.5	20.4
Stainless steel vessel	16.8	17.3

- Power density

There is also a very good agreement for the power density in the inner cable (cable1) along the magnet (Figure 2). The two longitudinal distributions show the same behaviour, with a discrepancy, within 15%, appearing at the end of the magnet.
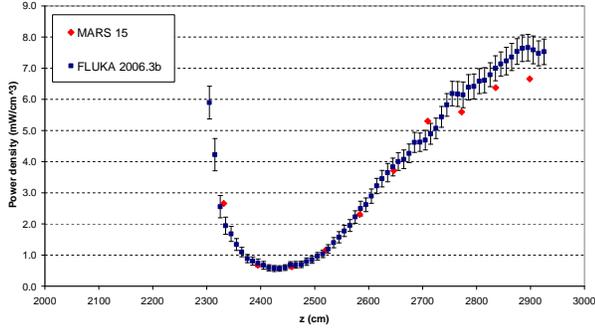

Figure 2: Azimuthally averaged power density in inner cable along the magnet.

- Particle spectra in the inner cable (cable1)

For particle spectra scored in the first superconducting coil (Figure 3: pions and kaons), the comparative results show small differences that can be explained by differences in the particle production models.
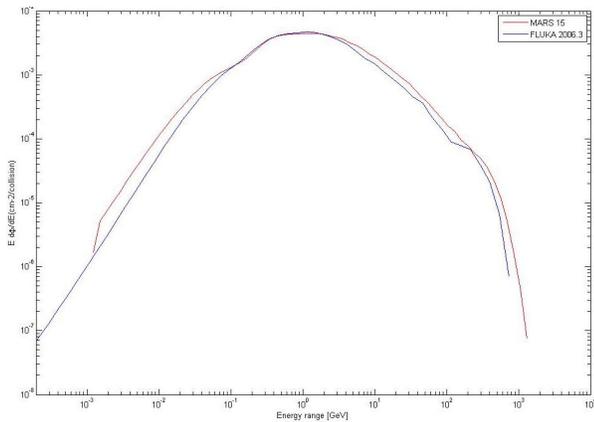

Figure 3: Pion & kaon spectra in cable1.

DETAILED MODEL FOR THE ENERGY DEPOSITION IN THE TRIPLET

Relying on the conclusive results of the inter-comparison work, a detailed model of the insertion region IR5 (CMS) for version 6.5 of the LHC layout has been performed with FLUKA [6] as was done earlier with MARS [6]. All essential components in the insertion region up to 60 m from the interaction point have been implemented with a detailed description of their geometry, material and magnetic field.

Detailed Geometry

The geometry has been described including details of the vacuum chambers along the insertion IR5 with the beam screens and the beam pipes. The geometry layout includes the TAS absorber in front of the inner triplet, the inner triplet composed of 4 superconducting magnets Q1 and Q3 (MQXA) and Q2a and Q2b (MQXB), the corrector magnets (MCBX, MQSX, MCBXA) and an absorber (TAS B) between Q2b and Q3 (Figure 4). The different colours represent different materials. The IP is located on the left side on Figure 4.

The proton-proton collisions have been modelled with a crossing half-angle (142.5 µrad) in the horizontal plane.
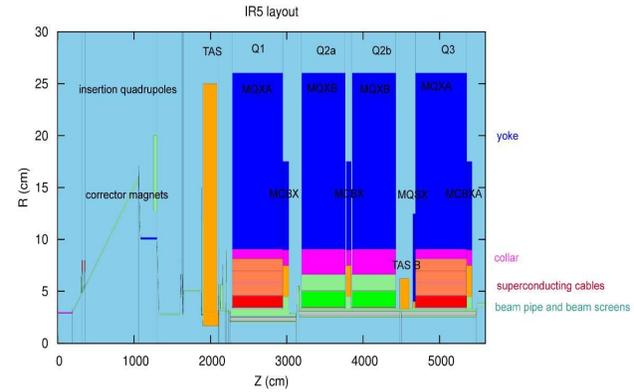

Figure 4: IR5 layout.

Energy Deposition Results

- Total Heat Loads

Table 2 gives the total heat loads in the inner triplet components. These integral values have a statistical error of less than 5%. The statistics include more than 10 000 proton-proton collisions. The total heat loads per magnet are between 20 and 30W for the baseline nominal luminosity of $L=10^{34} cm^{-2} s^{-1}$
.

Table 2: Total heat loads (W),
nominal luminosity $L=10^{34} cm^{-2} s^{-1}$

IR5 Elements	FLUKA	Statistical errors [%]
TAS	152.8	0.6
TAS B	4.0	3.8
Q1	28.6	0.6
Q2a	23.5	1.3
Q2b	23.5	1.0
Q3	25.8	0.7
Correctors	11.3	1.0

- Power density: longitudinal projection

Figure 5 shows the azimuthally averaged power density along IR5. We observe how the thick liner inside Q1 magnet efficiently shields the Q2a magnet.

- Effect of the magnetic fields

A large contribution to the power deposition in the magnets is due to low energy particles brought outside the

3

aperture by the magnetic field. Figure 6 shows the impressive impact of magnetic field on peak power density in the triplet coils. The values are the maximum power densities over the azimuthal direction. When the magnetic field is switched off, the 2 last quadrupoles present peak values significantly higher than those in the 2 first quadrupoles. This is an effect of the TAS shadow which for straight trajectories originating from the IP, extends over the first half of the triplet according to the TAS aperture.

The peak energy deposition on the front face of the coil of each magnet is due to accumulation of particles within the solid angle corresponding to the distance between the magnets.
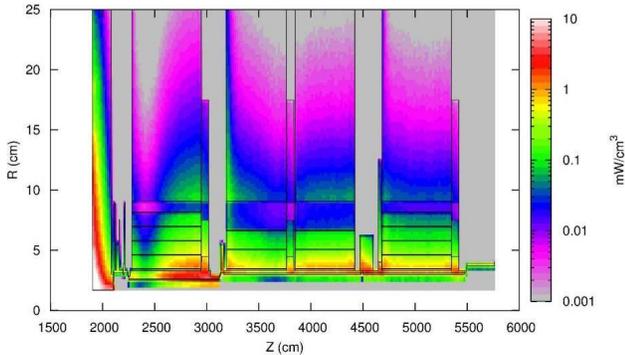

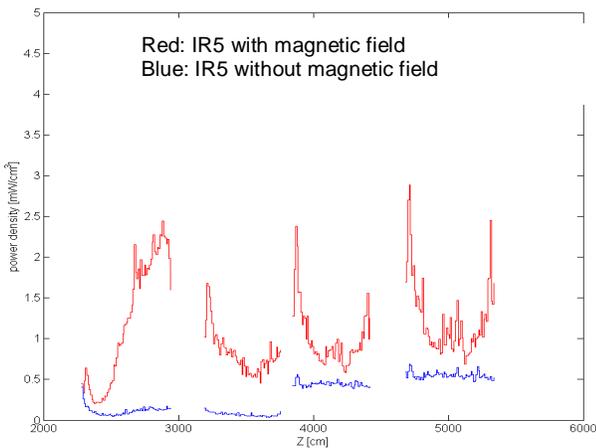Figure 5: IR5 azimuthally averaged power distribution.

Figure 6: Longitudinal distribution of peak power density in the inner cable for Q1 and Q3 (3.5<R<4.6 cm) and for Q2a and Q2b (3.5<R<5 cm), effect of the magnetic fields.

- Effect of the crossing angle

The power density distributions show some slight differences with and without the crossing angle of the beams (Figure 7). In Q1, with the crossing angle, the peak occurs in the horizontal plane at $0°$ (according to the outgoing beam direction), whereas with head on collisions, it occurs in the vertical plane at $90°$ (i.e. in the defocusing plane for positively charged particles). But the peak value remains the same, around 2.5 mW/cm3. With zero crossing angle, peak values along Q2b and Q3 are reduced.

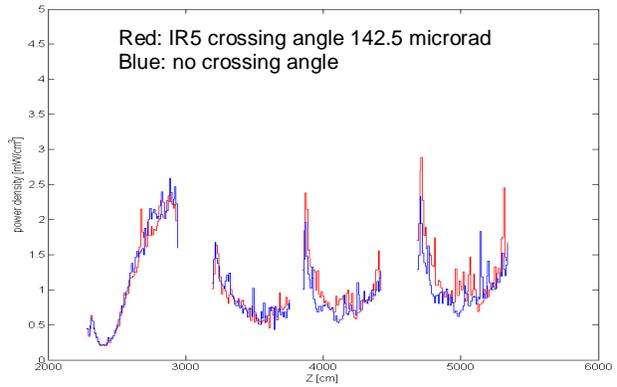Figure 7: Longitudinal distribution of peak power density in the inner cable for Q1 and Q3 (3.5<R<4.6 cm) and for Q2a and Q2b (3.5<R<5 cm), effect of the crossing angle.

CONCLUSIONS

An inter-comparison of FLUKA and MARS has been carried out using the same event generator for LHC proton-proton collisions. The energy deposition results came out to be in a good agreement.

The driving parameters of power deposition distribution have been addressed. The magnetic fields of the quadrupoles in the vacuum chambers have a large impact on the power deposition. They significantly increase peak power densities in the coils and total heat loads in the magnets with respect to the zero field case.

A crossing angle changes the location of the peak. Peak values are also slightly increased in the second part of the triplet, in comparison with the case of head on collisions.

The nominal operating conditions of the LHC have been looked at and the study confirms (see also results from [7]) that the peak power deposition complies with the 4 mW/cm^3 limit, which incorporates a safety factor of 3 on the quench limit for Nb-Ti Cable (12 mW/cm^3).

REFERENCES

[1] A. Fasso`, et al., *CERN Yellow Report* **2005-10** (2005).

[2] A. Fasso`, et al., in: "Computing in High Energy and Nuclear Physics 2003 Conference" (2003), arXiv:hep-ph/0306267.

[3] N.V. Mokhov, *Fermilab-FN* **628** (1995). http://www-ap.fnal.gov/MARS/.

[4] C. Hoa, N. Mokhov, F. Cerutti, A. Ferrari, *LHC Project Note* **411** (2008).

[5] S.Roesler, R.Engel, J.Ranft: "The Monte Carlo Event Generator DPMJET-III" in Proceedings of the Monte Carlo 2000 Conference, Lisbon, October 23-26, 2000, A. Kling, F. Barao, M. Nakagawa, L. Tavora, P. Vazeds., Springer-Verlag Berlin, 1033-1038 (2001).

[6] F. Cerutti, C. Hoa, E. Wildner, *LHC Project Report*, to be published.

[7] N.V. Mokhov, I.L. Rakhno, J.S. Kerby, J.B. Strait, *LHC Project Report* **633** (2003).